# JMEMS Letters

## Fabrication of Complex Structures on Nonplanar Surfaces Through a Transfer Method

Xuefeng Zeng and Hongrui Jiang

***Abstract*—We report on a method to fabricate complex microelectromechanical systems (MEMS) structures onto a flexible membrane. Three-dimensional and high-aspect-ratio MEMS structures were formed on a silicon-on-insulator wafer by deep reactive-ion etching and then were partially buried in a flexible polymer membrane. After being released from the silicon substrate, the flexible membrane with the complex structures could deform to curvilinear shapes and then could be transferred onto curvilinear surfaces. The effect of the structure and density of the pillars on the transferring procedure is studied. Potentially, this method could be utilized to transfer any MEMS structures and devices to any nonplanar surfaces, thus possessing great potential in MEMS devices. [2010-0286]**

***Index Terms*—Fabrication, flexible substrate, high aspect ratio, nonplanar surface.**

### I. Introduction

Micro/nanodevices on nonplanar or flexible surfaces have great applications but also present significant challenges [1]. The methods to implement micro/nanostructures and devices on nonplanar surfaces have been widely explored in recent years, including thin-film transistors [2], laser lithography on nonplanar surfaces [3], [4], flexible stamp [5]–[7], flexible bridge network [8], direct machining [9], and flexible mask on a cylindrical surface [1]. The thickness of the structures and devices implemented by these techniques is up to 2 $\mu$m, which is enough for electronic devices but significantly limits the applications for microelectromechanical systems (MEMS) devices. In this paper, we present a method to fabricate complex structures in a large area on nonplanar surfaces by utilizing a transfer method. Different sizes of 3-D and high-aspect-ratio MEMS structures and devices could be transferred to flexible membranes and could further be transferred to any nonplanar surfaces through this method.

### II. Mechanism

Fig. 1 shows the 3-D schematic of the deformation of a flexible polymer membrane with a complex MEMS structure partially buried in it. The square pillar array represents a high-aspect-ratio MEMS structure or device. After the fabrication of the planar MEMS structure, it is partially buried into a polymer membrane, formed surrounding it.

Manuscript received October 5, 2010; accepted November 21, 2010. Date of publication January 10, 2011; date of current version February 2, 2011. This work was supported by the U.S. National Science Foundation under Grant EFRI 0937847. Subject Editor J. A. Yeh.

X. Zeng is with the Department of Electrical and Computer Engineering, University of Wisconsin–Madison, Madison, WI 53706 USA (e-mail: xzeng2@wisc.edu).

H. Jiang is with the Department of Electrical and Computer Engineering, the Department of Biomedical Engineering, the Materials Science Program, and the Eye Research Institute, University of Wisconsin–Madison, Madison, WI 53706 USA (e-mail: hongrui@engr.wisc.edu).

Color versions of one or more of the figures in this paper are available online at http://ieeexplore.ieee.org.

Digital Object Identifier 10.1109/JMEMS.2010.2100034

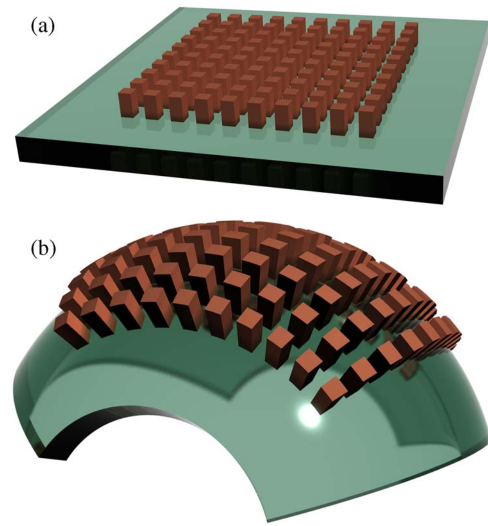


Fig. 1. Three-dimensional schematic of a flexible membrane with a partially buried MEMS structure. (a) Fabricated planar MEMS structure is partially buried in a planar but flexible membrane. (b) When the membrane deforms, the whole structure can change to any curvilinear shape following the membrane.

This polymer membrane is so thin and flexible that it can easily deform to any curvilinear shape. The MEMS structure could also deform to the same shape following the membrane while it would not have any damage or breaks.

### III. Fabrication Process

Fig. 2 shows the fabrication process flow of a pillar array transferred to a flexible membrane. Here, the pillars were formed on a silicon-on-insulator (SOI) wafer by deep reactive-ion etching (DRIE). The flexible membrane was a photoresist SU-8. All fabrication was executed in a clean room.

The fabrication process started from a SOI wafer (Silicon Quest International, Inc., Santa Clara, CA), as shown in Fig. 2(a). The silicon and the buried silicon oxide ($SiO_2$) layers are 60 and 2 $\mu$m thick, respectively. First, a $SiO_2$ layer that is 800 nm in thickness was thermally grown by wet oxidation at 1050 °C for 2 h, as shown in Fig. 2(b).

Then, a pattern was formed through photolithography, as shown in Fig. 2(c). Positive photoresist Shipley 1813 (MicroChem Corporation, MA, USA) that is 1.3 $\mu$m in thickness was spin coated and was patterned through photolithography. Next, the $SiO_2$ layer was etched in 6 : 1 buffered oxide etch (BOE) solution for 8 min, as shown in Fig. 2(c). Then, the silicon layer was etched using inductively coupled plasma (ICP) DRIE (Surface Technology Systems, Newport, U.K.) for 40 min to form a pillar array, as shown in Fig. 2(d). Both the photoresist and $SiO_2$ layers were used as the etching mask. The etching process included two types of cycles, pass cycles and etch cycles. Each pass cycle was 6 s, and the gas flow of octafluorocyclobutane ($C_4F_8$) was 12 standard cubic centimeters per minute (sccm). The power on the radio frequency (RF) coil and RF platen were 600 and 0 W, respectively. Each etch cycle was 11 s. The gas flow of sulfur hexafluoride ($SF_6$) and oxygen ($O_2$) were 130 and 13 sccm, respectively. The power on the RF coil and RF platen were 600 and 13 W, respectively. The

1057-7157/$26.00 © 2011 IEEE

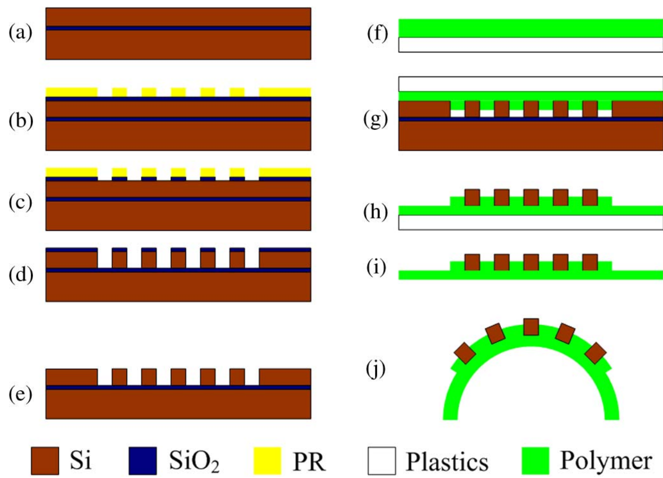


Fig. 2. Fabrication process flow of a pillar array partially buried in a flexible polymer membrane by the transfer method. (a) SOI wafer was used here, and two layers of Si and $SiO_2$ were 60 and 2 $\mu$m thick, respectively. (b) $SiO_2$ layer of 800 nm was thermally grown. The patterns were formed through photolithography. (c) Top $SiO_2$ layer was wet etched in 6 : 1 BOE solution for 8 min. (d) Si was etched by ICP DRIE for 40 min to form a pillar array. (e) Thickness of the top $SiO_2$ layer was reduced to around 300 nm after DRIE. The remaining mask $SiO_2$ layer was removed in 6 : 1 BOE solution for 4 min. (f) 50-$\mu$m-thick layer of photoresist SU-8 2050 was spin coated onto a plastic sheet. (g) Plastic sheet with SU-8 was attached onto the etched SOI wafer and was baked at 105 °C for 1 min. SU-8 was subsequently cured under a flood exposure for 5 min. (h) Plastic sheet with the attached pillar array was placed in 6 : 1 BOE solution for 24 h to etch the buried $SiO_2$ layer. (i) Removal of the plastic sheet. (j) Polymer membrane with the pillar array was formed and could deform to a curvilinear shape.

buried $SiO_2$ layer was used as the etch-stop layer. After etching, the thickness of the top $SiO_2$ layer was reduced to around 300 nm. This $SiO_2$ layer was removed in 6 : 1 BOE solution for 4 min, as shown in Fig. 2(e).

Subsequently, another layer of photoresist SU-8 2050 (MicroChem Corporation, Newton, MA) was spin coated onto UV-transparent polyethylene terephthalate that is 127 $\mu$m in thickness (Melinex ST505, DuPont Teijin Films, DuPont, Wilmington, DE), as shown in Fig. 2(f). The thickness of SU-8 was 50 $\mu$m. Next, SU-8 was attached onto the pillar array and was baked at 105 °C for 1 min. Subsequently, it was cured under a flood UV exposure for 5 min. The pillar array was partially buried into the SU-8 polymer membrane, as shown in Fig. 2(g). The buried $SiO_2$ layer was etched in 6 : 1 BOE solution for 24 h to release the polymer membrane with the pillar array, as shown in Fig. 2(h). Finally, the polycarbonate sheet was also peeled off from the SU-8 membrane, as shown in Fig. 2(i). This membrane was flexible and could deform to any curvilinear shape, as shown in Fig. 2(j).

## IV. Experimental Results

Different sizes of structures were transferred through this method. Fig. 3 shows the scanning electon microscope (SEM) images of three kinds of pillar arrays etched by DRIE, hexagon, square, and triangle. The height of all pillars is the same as the thickness of the silicon layer, which is 60 $\mu$m. The side lengths of both the outside hexagon and the inside square are 30 $\mu$m. The distance between the centers of any two neighboring hexagons is 100 $\mu$m. The side lengths of the outside and inside squares are 100 and 50 $\mu$m, respectively. The distance between the centers of any two neighboring squares is 150 $\mu$m. The side length of the triangle is 26 $\mu$m. The distance between the centers of any two neighboring triangles is 39 $\mu$m. Ignoring the

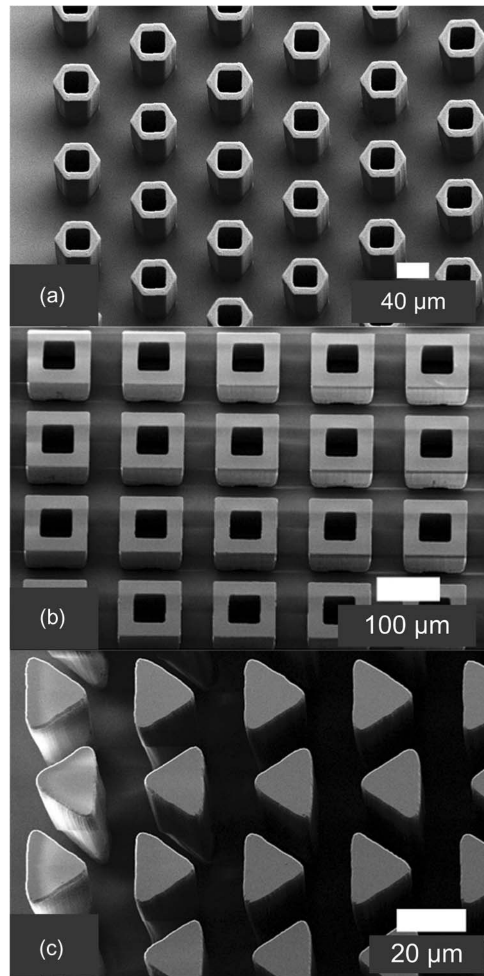


Fig. 3. Images of three kinds of pillar arrays after DRIE. The height of all pillars is defined by the silicon layer to be 60 $\mu$m. SEM images of (a) hexagon array, (b) square array, and (c) triangle array.

holes in the hexagon and square arrays, the triangle array has the highest pillar density with 1139 pillars/mm$^2$. The square array has the lowest pillar density and consists of 44 pillars/mm$^2$. The hexagon has 115 pillars/mm$^2$.

Fig. 4(a) and (b) shows the optical and SEM images of the flexible polymer membrane with the square array, respectively. All polymer membranes with the arrays were successfully attached to a hemispherical dome with a diameter of 25.2 mm. The array consisted of 40 × 40 pillars, and the total size was 6 × 6 mm$^2$. Fig. 4(c) and (d) shows the images of the membrane with the square array on the hemispherical dome. Fig. 4(e) shows the image of that membrane with large depth of focus (DoF) combined from multiple images at different focal planes taken by a Nikon LV100 microscope (Nikon Engineering Co., Ltd., Japan). The total DoF was 1 mm, and the moving interval between the focal planes was 40 $\mu$m. Fig. 4(f) and (g) shows the images of the membranes with the hexagon array and the triangle array, respectively.

A large number of pillars have been transferred onto the flexible membranes with large areas without any damages of the pillars. The transferring yield is affected by the combination of the array density and the pillar structure. Comparing with the triangle array, the square and hexagon arrays had the higher yield. The first reason is the lower pillar density of the square and hexagon arrays. Because the size of the pillars and the gap between the pillar structures are large, which

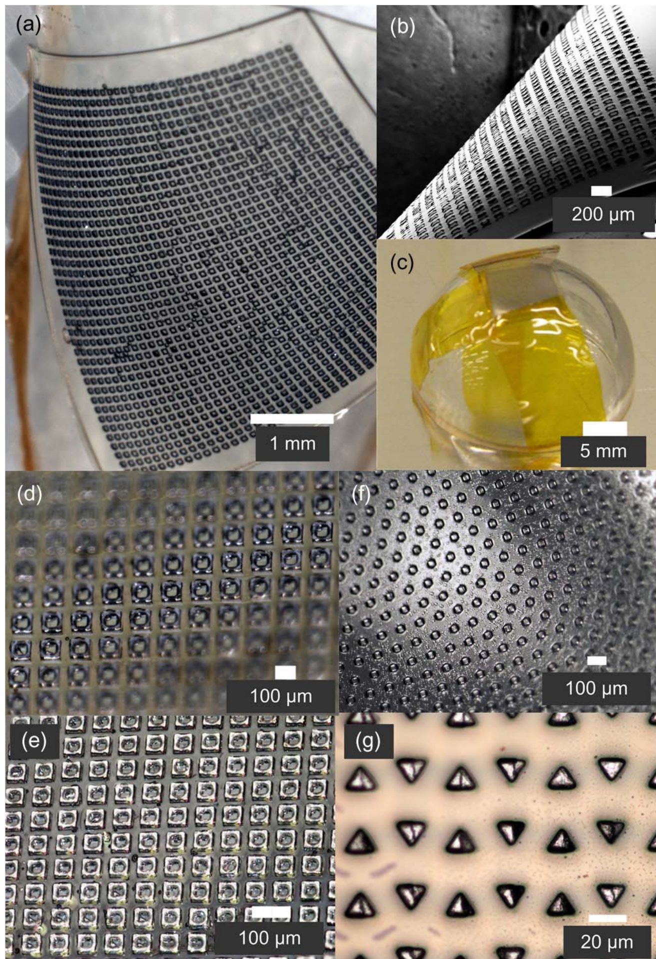


Fig. 4. Images of the pillar arrays partially buried in the flexible membranes. (a) Optical and (b) SEM images of the polymer membrane with the square array. (c) Image of the membrane with the square array on a hemispherical dome. (d) Optical image of the membrane with the square array on the dome. (e) Optical image of the membrane with the square array on the dome by combining multiple images at different focal planes along the optical axis for extended DoF. Images of the membranes (f) with the hexagon array and (g) with the triangle array on the dome.

means lower array density, the prepolymer fluid easily flows into the gaps and surrounds the pillars. On the other hand, for the structure with higher array density, air bubbles between the gaps tend to prevent the prepolymer fluid from entering the gaps, therefore reducing the transferring yield. In addition, the holes in the square and hexagon arrays also contribute to the increase in the transferring yield since the prepolymer fluid could flow into the holes and thus increase the adhesion.

## V. Conclusion

In summary, we have demonstrated a method to fabricate complex MEMS structures transferred to a flexible membrane in a large area. Three kinds of pillar structure arrays with different array densities have been successfully transferred to flexible polymer SU-8 membranes. The transferring yield is decided by the combination of the array density and the pillar structure. Potentially, this method could transfer any MEMS structures and devices to any nonplanar surfaces, thus possessing great potential in MEMS devices, particularly for optoelectronic and photonic devices.

In the future, the effect of the structures and the density on the transferring yield will be studied further. Aside from SU-8, other photoresists with different thicknesses and other flexible membranes, such as polydimethylsiloxane, will be used as the transferring membranes. Such a transferring method can also be applied to removable polymer membranes, thus allowing multiple transferring procedures, so that MEMS structures ultimately can be transferred onto different kinds of curvilinear surfaces and substrates. Each component in the array could also be connected together by using a flexible polymer bridge structure [8]. The shape of membranes would be optimized to reduce the stress from deformation.

## Acknowledgment

The authors would like to thank C.-W. Lo for the assistance in taking SEM images. The authors would also like to thank Prof. J. Rogers and his research group at the University of Illinois at Urbana–Champaign, and Dr. D. Cheng, C. Li, and D. Zhu for the discussions and help. This research utilized National Science Foundation-supported shared facilities at the University of Wisconsin.

## References

[1] W. J. Li, J. D. Mai, and C. M. Ho, "Sensors and actuators on non-planar substrates," *Sens. Actuators A, Phys.*, vol. 73, no. 1/2, pp. 80–88, Mar. 9, 1999.

[2] R. A. Street, "Thin-film transistors," *Adv. Mater.*, vol. 21, no. 20, pp. 2007–2022, May 25, 2009.

[3] M. Mizoshiri, H. Nishiyama, J. Nishii, and Y. Hirata, "Silica-based microstructures on nonplanar substrates by femtosecond laser-induced nonlinear lithography," *J. Phys., Conf. Ser.*, vol. 165, no. 1, p. 012048, Jun. 10, 2009.

[4] D. Radtke and U. D. Zeitner, "Laser-lithography on non-planar surfaces," *Opt. Express*, vol. 15, no. 3, pp. 1167–1174, Feb. 5, 2007.

[5] R. J. Jackman, J. L. Wilbur, and G. M. Whitesides, "Fabrication of submicrometer features on curved substrates by microcontact printing," *Science*, vol. 269, no. 5224, pp. 664–666, Aug. 4, 1995.

[6] H. C. Ko, M. P. Stoykovich, J. Z. Song, V. Malyarchuk, W. M. Choi, C. J. Yu, J. B. Geddes, J. L. Xiao, S. D. Wang, Y. G. Huang, and J. A. Rogers, "A hemispherical electronic eye camera based on compressible silicon optoelectronics," *Nature*, vol. 454, no. 7205, pp. 748–753, Aug. 7, 2008.

[7] M. M. Roberts, L. J. Klein, D. E. Savage, K. A. Slinker, M. Friesen, G. Celler, M. A. Eriksson, and M. G. Lagally, "Elastically relaxed free-standing strained-silicon nanomembranes," *Nat. Mater.*, vol. 5, no. 5, pp. 388–393, May 2006.

[8] D. F. Zhu, C. H. Li, X. F. Zeng, and H. R. Jiang, "Tunable-focus microlens arrays on curved surfaces," *Appl. Phys. Lett.*, vol. 96, no. 8, p. 081111, Feb. 2010.

[9] K. Takahata, S. Aoki, and T. Sato, "Fine surface finishing method for 3-dimensional micro structures," in *Proc. IEEE 9th Annu. Int. Workshop MEMS—An Investigation of Micro Structures, Sensors, Actuators, Machines Systems*, San Diego, CA, Feb. 11–15, 1996, pp. 73–78.